NUMERICAL 3D ANALYSIS OF A MINI WIND TURBINE WITH HORIZONTAL AXIS, FOR IMPLEMENTATION IN AGRICULTURAL FARMS
/
ANALIZA NUMERICA 3D A UNEI TURBINE EOLIENE DE PUTERE MICA CU AX ORIZONTAL IN VEDEREA IMPLEMENTARII IN FERMELE AGRICOLE

George Ipate[1], Gabriel Alexandru Constantin[1], Sorin Ștefan Biris[1],
Gheorghe Voicu [1], Carmen Otilia Rusanescu [1], Vasilica Ștefan [2]
[1] Universities Polytechnic Bucharest, Faculty of Biotechnical Systems Engineering / Romania
[2] National Institute for Research-Development of Machines and Installations Designed for Agriculture
and Food Industry - INMA Bucharest / Romania
Tel: 0766445321; E-mail: puiu.ipate@gmail.com
DOI: https:// doi.org/10.35633/inmateh-62-34

ABSTRACT

The purpose of this paper is the numerical study of the effects of the fluid interaction with the blades of the working bodies of the renewable energy conversion systems. The paper presents the results of numerical research regarding the influence of the blade shape (straight), the number of blades (2, 3, 4) or the wind speed in the area on the output power of the small capacity wind turbines. The validation of the simulation data was performed by comparison with the experimental data obtained on a Windtrainer Junior laboratory wind energy system. Computed power coefficients are in good agreement with the experimental results. Increasing the efficiency of energy conversion for small wind turbines for their implementation in green farms represents a significant step in the concept of sustainable rural development.

REZUMAT

Scopul acestei lucrări este studiul numeric al efectelor interacțiunii fluidului cu lamele corpurilor de lucru ale sistemelor de conversie a energiei regenerabile. Lucrarea prezintă rezultatele cercetărilor numerice cu privire la influența formei lamei (drepte), numărul de pale (2, 3, 4) sau viteza vântului în zona pe puterea de ieșire a turbinelor eoliene de mică capacitate. Validarea datelor simulate a fost efectuată prin comparație cu datele experimentale obținute pe un sistem de energie eoliană de laborator Windtrainer Junior. Coeficienții de putere calculați sunt în acord cu rezultatele experimentale. Creșterea eficienței conversiei energiei pentru turbinele eoliene mici pentru implementarea lor în ferme ecologice reprezintă un pas semnificativ în conceptul de dezvoltare rurală durabilă.

INTRODUCTION

The need to reach a higher standard of living and increase the world's population have produced a dramatic increase in energy consumption globally. All energy sources affect the environment to a greater or lesser extent. There is no completely "clean" power source. Most of our energy comes from 85% fossil fuels - coal, oil and natural gas, and the burning of these fuels causes pollution of the environment in which we live. To reduce the long-term impact of the energy industry on the environment, strategies are developed and implemented to increase the efficiency of energy use, to capitalize on alternative sources and on sustainable development.

Wind energy is one of the renewable energy sources that can be harnessed due to its quite good potential. Generating small scale electricity is closer to the final user, significantly reducing transport losses. This leads to lower energy costs for consumers and ensures greater efficiency. In isolated areas, where electricity grids are missing or are isolated and have low transport capacity, individual turbines or small groups of turbines of different sizes are located. Small-scale electricity generation can be considered to be more reliable, cheaper, more efficient and more environmentally friendly than centralized production.

The ability of modern computing systems to operate quickly with a large volume of data offers the unique opportunity for researchers to investigate problems whose practical approach would be too costly, long-lasting or even impossible. Thus, the researcher can obtain optimal technical solutions that approach the experimental reality in a reasonable time.

Mara et al., (2014), study a model for aerodynamics simulation of Magnus wind rotor blades using Ansys CFX. They evaluated various strategies for obtaining the grid and models of turbulence to accurately validate the model in relation to the experimental data published by *Bychkov et al. (2007). Rogowski et al., (2017),* performed a numerical analysis of a small-size vertical-axis wind turbine performance. They developed a two-dimensional model of vertical-axis wind turbine based on the experimental Darrieus wind turbine, and show that velocity profile becomes more asymmetric in relation to upper tip speed ratios if the rotor is operating at lower tip speed ratios.

Nigam et al., (2017), perform a CFD analysis of a Vestas V82-1.65 MW horizontal axis wind turbine blade and NACA 634 -221 airfoil profile of wind turbine using k-SST turbulence model in Ansys Fluent. The results obtained for the traction coefficient and the moment of depositing at different angles of attack or lift coefficient are compared with the experimental results and show a good correlation. They also concluded that the air velocity is higher on the upper surface of the wing, while the air pressure on the lower surface of the wing is also increased.

Wenehenubun et al., (2015), studied the performance of Savonius wind turbines related with the number of blades. For this work the ANSYS 13.0 software simulations were used to show the pressure distribution of wind turbine. *Wußow et al., (2007),* studied the airflow around a wind turbine (WT) of the type Enercon E66 with emphasis on the turbulent wake by using CFD simulations. It was found that the local values of turbulence intensity and the amplitude of the velocity inside the trace fits quite well with the measurements. *Bose et al., (2014),* studied numerically, using a commercial CFD code, the effect of pitch angle on the performance of a three bladed straight H-Darrieus vertical axis wind turbine. They showed that the presence of vortices close to the trailing edge deteriorates the performance of the turbine.

The main purpose of the present paper is the theoretical and experimental argumentation of the aerodynamic characteristics of a wind turbine in the aspect of increasing the energy conversion efficiency for low power wind turbines. In order to achieve the formulated purpose, CFD simulations were performed for different wind speeds to determine the performance factor of the developed rotor and the aerodynamic forces acting on the blade, or to model the fluid's interaction with the blade structure to verify the resistance of the blade in stationary regime.

MATERIALS AND METHODS

The wind turbine works due to the difference of forces exert on each blade according to *Wenehenubun, (2007).* The maximum power of wind turbine P_t is determined as:

$$P_t = T \cdot \omega \ \text{[Watt]} \tag{1}$$

where:

T is the torque (Nm) and ω is the angular velocity of rotor (s^{-1}).

The performance of wind turbine can be expressed in the form of torque coefficient (C_t) and the coefficient of power (C_p). The tip speed ratio or $TSR\ (\lambda)$ is a parameter related with rated wind speed and rotor diameter. As the ratio between the speed of tip blade and wind speed through the blade, TSR can be determined with relation (2) according to *Hameed and Afaq, (2013):*

$$\lambda = TSR = \frac{V_{rotor}}{V} = \omega \cdot d / V \tag{2}$$

where:

V_{rotor} is the tip speed or the peripheral velocity of rotor (m/s), V is the wind speed (m/s) and d is the diameter of the rotor (m). The coefficient of torque or C_t is defined as the ratio between the actual torque develop by the rotor (T) and the theoretical torque available in the wind (T_w) as,

$$C_t = \frac{T}{T_w} = \frac{4T}{\rho_{air} \cdot d \cdot A_s . V^2} \tag{3}$$

where:

ρ_{air} is the density of air (kg/m^3) and A_s is the swept area of blades (m^2). The power coefficient of a wind turbine (C_p) can be determined from the ratio between the maximum power obtained from the wind or the mechanical (P_t) and the total power available from the wind (P_w),

$$C_p = \frac{P_t}{P_w} = \frac{P_t}{0.5 \cdot \rho_{air} \cdot A . V^3} \tag{4}$$

The relationship between the power coefficient C_p and the tip speed ratio λ is an effect of solidity of the wind turbine performance. The electric power produced by wind turbine is computed from the relation:

$$P_e = \eta_b \cdot \eta_m \cdot \eta_e \cdot P_w \qquad (5)$$

where: η_b is blade aerodynamic efficiency, η_m is mechanical efficiency and η_e electrical efficiency.

| a) | b) | c) |
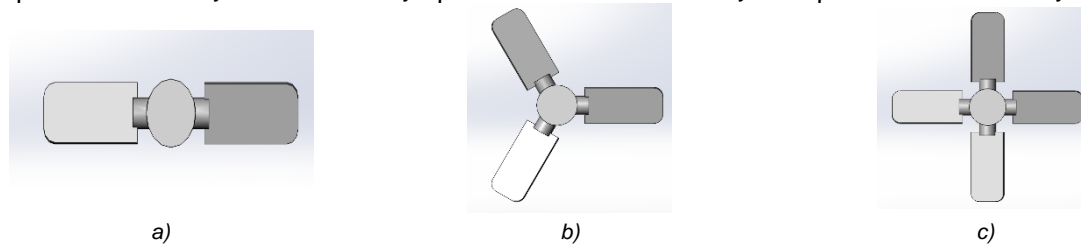
Fig. 1 – Blade profile and rotor geometry
a) 2PalDREP; b) 3PalDREP; c) 4PalDREP

The experiment used a wind turbine model with two, three and four straight blades (with acronym 2PalDREP, 3PalDREP and 4PalDREP), as shown in Fig. 1. The dimensions of the blades of the wind turbine model are length = 40mm, width = 20mm, thickness = 2mm, angle of attack of the profile α= 15 degrees, rotor diameter = 110mm. The model of wind turbine was performed in an open circuit wind turbine as shown in Fig. 2. The controllable wind machine (low voltage) was started to produce wind and an anemometer measured the velocity of wind. When the wind produced by the centrifugal fun pushed the blades of the model, the rotor of wind turbine will rotate. Each experiment with two, three and four blades respectively used the speed of wind from 4.5 to 12.5 m/s. The power of the generator depending on the wind force was measured using the 2 multimetres (U-volt / I-ampere) with 2 mm connectors.

ANSYS Workbench platform was used for numerical modelling. For the dynamic calculation of fluid flow, the Ansys - CFX5 module was used. The three-dimensional geometry was realized in the computer-aided design program SolidWorks 2016 and subsequently exported to the DesignModeler program in the Workbench environment.

Fig. 2 – The experimental laboratory system Windtrainer Junior

In the pre-processing phase, the calculation domain was created as follows: a stationary domain consisting of a rectangular parallelepiped of length L=0.45m, height H=0.14m and width B=0.13m over which a semicylinder whose radius is superposed is R=0.065m; a rotational domain having a cylindrical shape with a height of H_c=0.01m or the radius of the turbine and a radius of the base R_b=0.08m. The fixed domain is obtained by the operation of removing the cylinder and the assembly: turbine support block (a rectangular parallelepiped with dimensions L_b=0.12m, H_b=0.04m, B_b=0.08m) tower turbine (a cylinder with dimensions D_t=0.02m, H_t=0.08) and turbine platform (a cylinder with dimensions D_n=0.04m, H_n=0.06m) from the stationary domain. The two domains are connected topologically by the surface of the cylinder having a double grid on its surface (non-conforming interface), one coming from the fixed domain and another coming from the rotating domain. To avoid unwanted interpolation errors when moving from one computing domain to another, the size of the elements at the interface is approximately the same on both sides of the cylinder.
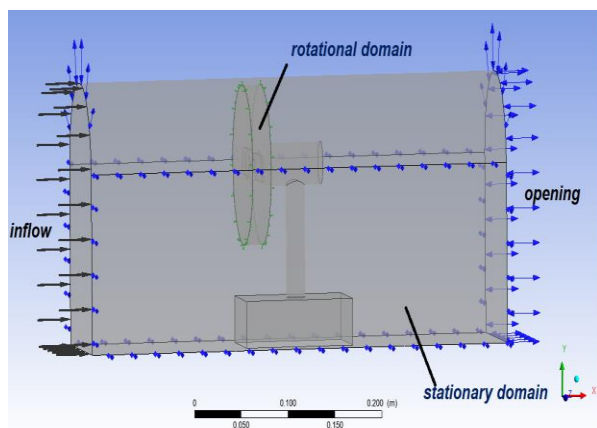
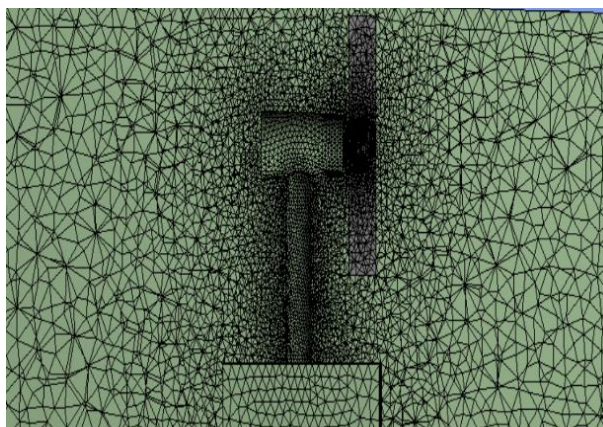**Fig. 3 - Detail domain and boundary conditions**   **Fig. 4 – Model discretization**

Figure 4 shows the discretized domain and the level of refinement of the network in the rotor region. The calculation grid was created in the Ansys Mesh program that allows the creation of grids with refined tetrahedral elements by halving the sides of the elements. For all the calculation scenarios, the same computing network (grid) was used, consisting of 417969 elements and 77217 nodes, distributed as follows: 261544 elements and 47647 nodes in the grid associated with the fixed domain and 156425 elements and 29570 nodes for the grid in the rotating domain. The boundary conditions applied to the simulation are shown in figure 3.

The assumptions made in setting the calculation case can be summarized as follows:
- the flow is completely turbulent on the blade and the nacelle;
- the infinite upstream current is uniform and has a speed of 4.5 - 12.5 m/s;
- at infinite upstream the turbulence fluctuations have an intensity of 5% compared to the average speed;
- at infinite upstream the pressure is constant and equal to 1 atm, idem temperature is 288.15K.
- the flow is a stationary one, although we have rotation, the formed slope has a periodic character, and the aerodynamic coefficients do not vary after a certain period.

Current cases required approximately 10.5GB RAM, and the simulation time for convergence (decreasing residuals by 5 orders of magnitude and stabilizing aerodynamic coefficients) on a dual-core processor at 2.6 GHz took more than 15.2 hours.

RESULTS

In this paper, the results obtained from the flow simulations carried out for the turbine with two, three and four straight blades are presented below. The simulations were performed for a speed ratio at the tip of the blade (TSR) of 0.026, at the air inlet speed of 6.9 m/s, and a power coefficient Cp = 0.00342 for the 2-blade model, Cp = 0.02843 for the model with 3 blades, respectively, $Cp4$ = 0.06764 for the 4 blade model. The very low coefficient of power made us investigate the possibility of using the protective cap as an element of limiting the effect of the "infinite extent" that leads to the decrease of the load and the appearance of the induced resistance, factors that decrease the aerodynamic momentum.

The power coefficient curve obtained from the CFD results is compared with the experimental data obtained, the numerical results for the power coefficient curve showing a fairly good agreement with the experimental data. The simulation results include velocity distribution, pressure distribution along the flow direction, turbulent kinetic energy distribution behind the wind turbine and turbine power.

Because the ratio of the speed to the blade type is dependent on the angular velocity and the wind speed, the angular velocities are unchanged in each run, because the design is simulated at the constant wind speed. In order to obtain the aerodynamic properties of the model, the lifting and traction forces, the calculation function from the results processing file from Ansys CFX was used. Thus, the normal force along the X axis, which is equivalent to the lifting force, and the normal force along the Z axis, which is equivalent to the tensile force, were obtained. Similar results were reached by *Mara et al., (2014)*.

a)   *b)*   *c)*
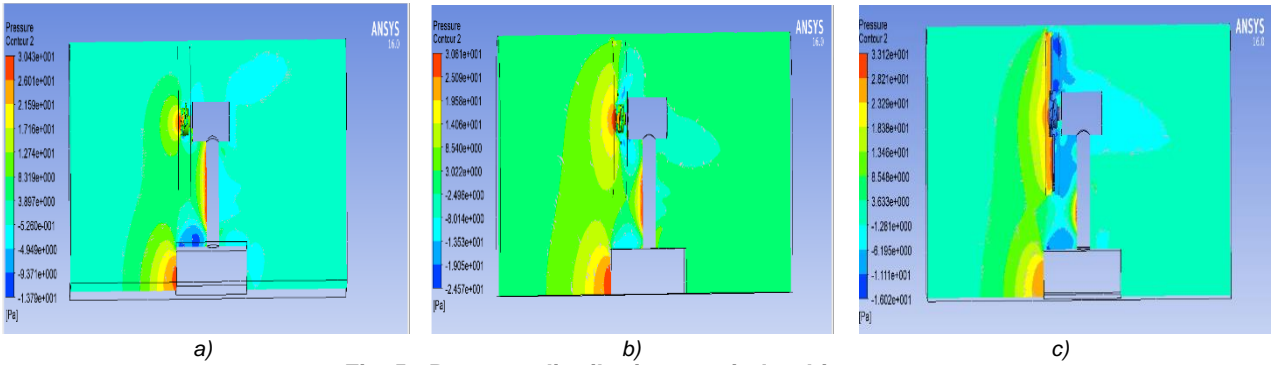
Fig. 5 - Pressure distribution on wind turbine rotor
a) two blades; b) three blades; c) four blades

Fig. 5 shows pressure distribution for wind turbine rotor with two blades (a), three blades (b) and four blades (c). Pressure on four blades is higher than pressure on two and three blades with result that the deviation of drag forces will rotate the rotor. As shown in Fig. 5 (a) and (b), pressure in front of the blades is higher than that at the back and wind turbine rotor will rotate. The pressure differences between the front area and the back of the wind turbine blades are clearly outlined in Fig. 5 (c). This makes the four-blade wind rotor have the highest torque compared to the other types of wind turbine rotors.

Figure 6 gives a snapshot of the unsteady turbulent wake and show contour plots of velocity magnitude ranging from 0 to 7.6 m/s. Blue areas denote areas of very low wind speed in the vicinity of the walls and close downstream of the tower, as *Wußow (2007)* found it too. Distribution of pressure on both sides, top and bottom, contributes to the lift. Pressure drag is the part of drag force connected to the pressure distribution around the airfoil, as *Nigam et al., (2017)* and *Bose et al., (2014)* described too. In accordance with those found by *Jang et al. (2019),* as the pressure of the fluid increases, the flow velocity decreases, resulting in the lowest value inside the rotor and the maximum value on the outer surface.

Figure 7 shows the evolution of the turbulence kinetic energy for the three types of rotors since the beginning of the wind action on the blade, for values of the wind speed considered of 6.9 m/s. It is noted: the lower the stabilized flow velocity of the fluid, the turbulence intensity initially has higher bursts, but they occur later than those produced at higher speeds, and the stabilization of the turbulence intensity occurs at higher values and with more pronounced oscillations.

a)   *b)*

c)
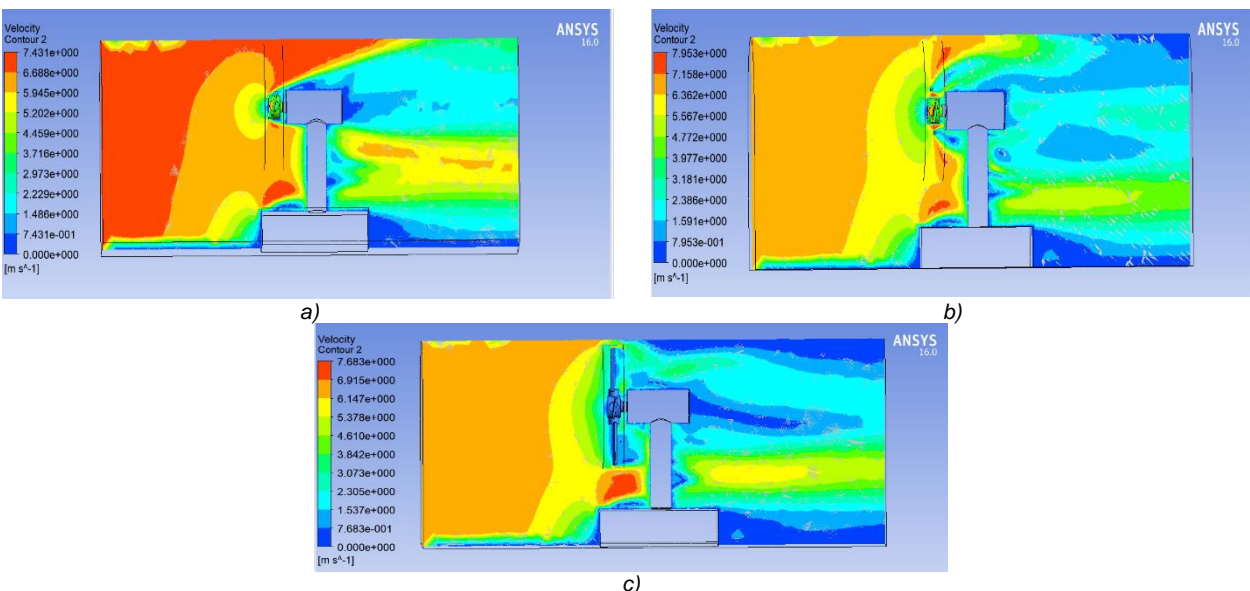
Fig. 6 - Contours of air velocity magnitude in plane section at an input speed of 6.9 m/s
a*) two blades; b) three blades; c) four blades*

The intensity of the turbulence, for the values of the fluid current acting on the blade, is in the range (0÷1.87) m²/s², which is considered to be low values, so a rather small value of the intensity of the turbulence (*Tudor, 2015)*. With this help you can see the areas with the highest potential for hydrodynamic losses, in

which the energy of the fluid is consumed unnecessarily. In the detail of figure 7 b) and c) an area of maximum kinetic energy is highlighted, which appeared at the interface between the stationary and the rotational zone, due to the existence of a very small intersection.
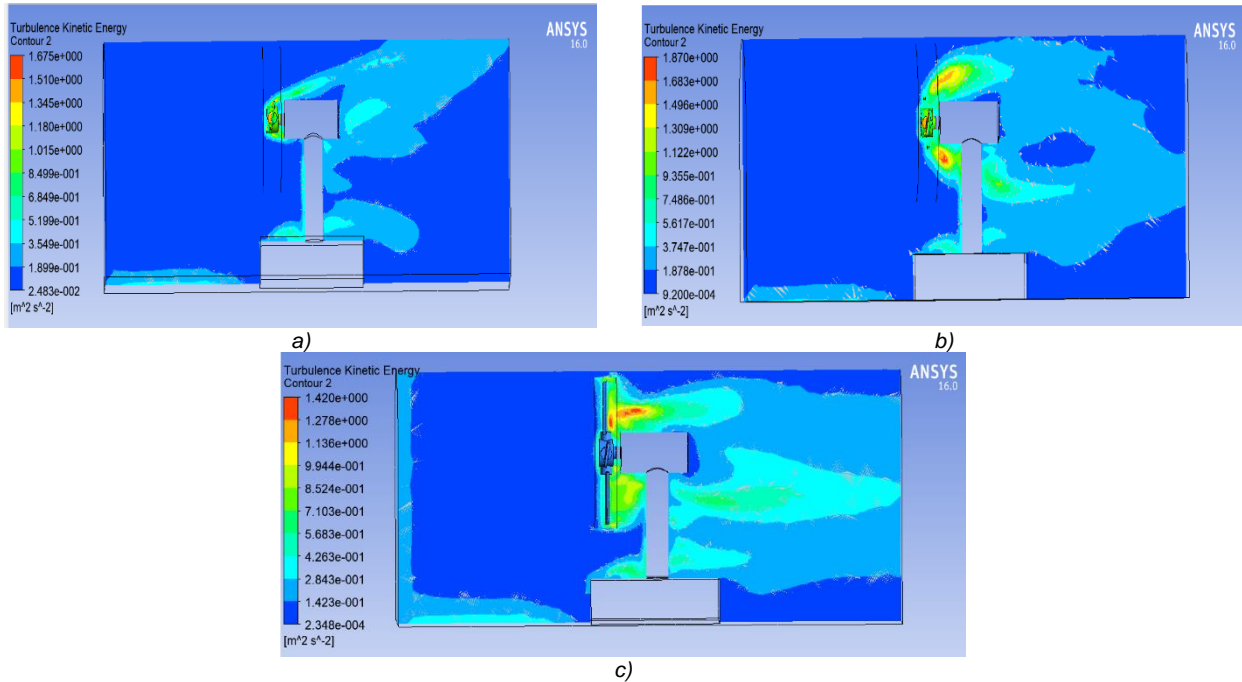

a)

b)

c)

Fig. 7 – Turbulence kinetic energy distribution
a) two blades; b) three blades; c) four blades

The representations of the temporal evolutions of the analysed parameters (static pressure, air velocity after the impact with the turbine blade, turbulence intensity, for wind speeds between 4.5 - 12.5 m/s) show that the disturbances introduced by them behind the turbine rotor are manifested more pregnant to a distance of 0.23 m.

During operation the wind turbine rotor is required at variable wind speeds that cause centrifugal forces and shear strength forces that bend the blade tip. The maximum aerodynamic forces for the wind speed of 6.9 m/s were determined using the CFX module to check the blade resistance. Then, these forces were transferred to the Structural analysis module with which the structural analysis of the blade was performed. The hub blade was fixed to the base by means of a rotational joint and required with aerodynamic forces distributed over its entire surface. The axial component of the aerodynamic forces was obtained by approximately 0.116823 N. Regarding the values of lift and traction coefficient, they were very small for all the tip speed ratios, which can lead to a significant average error. Figure 8 illustrates the pressure distributed over the entire surface of the blade in the form of vectors.
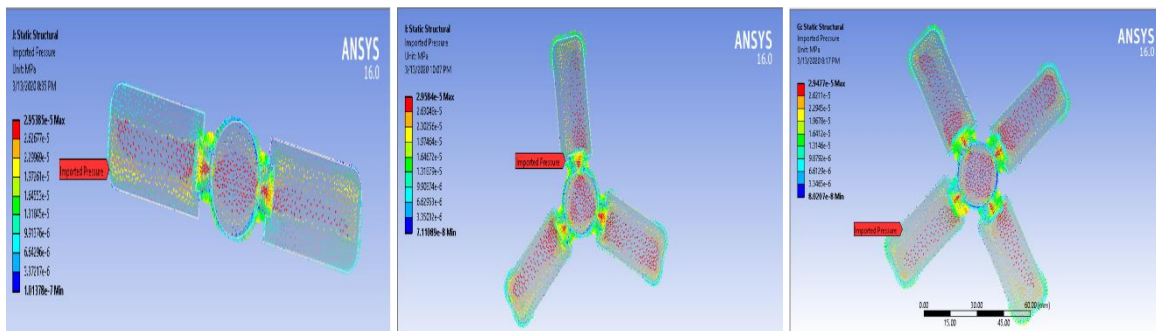

Fig. 8 – Distribution of pressure on rotor blades

The purpose of the structural analysis is to check the rigidity of the blade, to determine the stresses that appear in the blade as well as the moment of rotation, *as Paulesn et al (2013)* analyse too.

The 2-blade rotor has been discretized into 5999 nodes and 27330 elements, the 3-blade rotor into 8309 nodes and 37572 elements, respectively, the 4-blade rotor into 10152 nodes and 45585 finite elements, and the results of the static blade analysis are shown in Fig. 9. It can be easily observed that the maximum Von Mises equivalent stress appear when the blades are embedded in the rotor hub and have values in the range 2.1845e-002 MPa - 2.8533e-002 MPa.
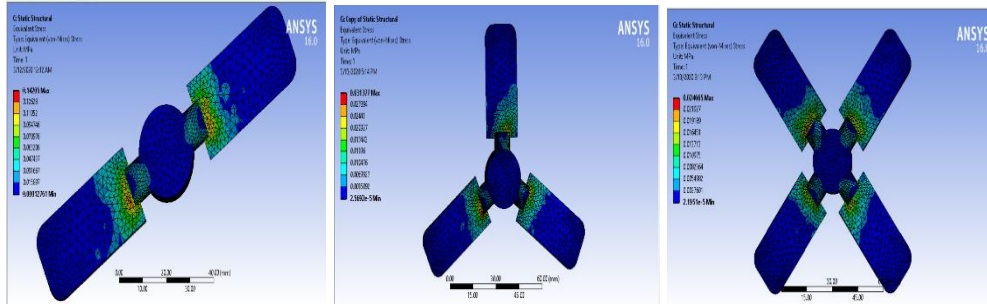

Fig. 9 - Distribution of Von Mises equivalent stress on rotor blades

For the validation of model and solution methodology the numerical predictions of coefficient of power Cp have been compared with the experimental results. The simulations have been done using the methodology described in the previous section, and Cp is plotted against wind speed V [m/s] as shown in Fig. 10. At very lower values of TSR (λ>0.026) the numerical predictions over predict the experimental values. This is in contradiction with those observed in the numerical predictions of *Bose et al., (2014).* In contrast, although all numerical results show similar trends, they vary significantly. The largest deviations are observed in figure 10 between Cp curves (*computed* - black line and *experimental* - green dot line) obtained for the 4-blades model and can be attributed to the 3D effects and the strong interaction of the blades with the vortices as well as to the considered turbulence model.

The aerodynamic power, also known as the power coefficient, in figure 10 was calculated using Equation (4). In case of experimental power coefficient, we need to consider external environmental condition, such as electrical losses and overspeed protection, which alter the torque-speed schedule of the generator and finally the turbine power performance.
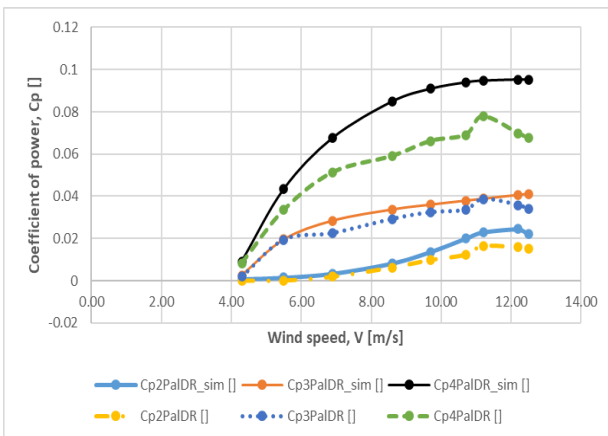

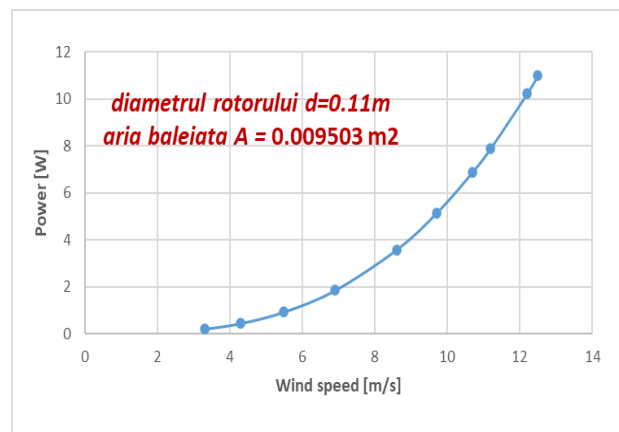
Fig. 10 – Coefficient of power vs. wind speed

Fig. 11 – The power curve of the turbine depending on the wind speed

In order to make a comparative analysis of the conversion capacity of the turbine with the existing rotor, the power curve was calculated (Fig. 11), without considering the mechanical losses.

CONCLUSIONS

Based on the CFD numerical simulations of the turbine rotor:

- the dimensions of the computational domain of the fluid were chosen so as to ensure the free flow without influencing the domain boundaries;

- the torque moments developed at the rotor shaft and the wind pressure distribution on the surface of the blade were determined for different wind speeds (4.5 - 12.5 m/s);

- the power curve was calculated, without considering the mechanical losses, and compared with the results of the experimental researches performed for this turbine;

- the resistance structure of the blade was checked in for the wind speed limit of 6.9 m/s - based on the simulation results of the fluid interaction with the blade structure;

- an area of maximum turbulent kinetic energy was highlighted, which appeared when the fluid interacted with the rotor blades and where the areas with the highest potential can be observed of aerodynamic losses, in which the energy of the fluid is consumed.

It was found that, as expected, the rotor of the four-blade wind turbines has a higher torque compared to the rotor of the two or three blades

REFERENCES

[1]　Bose, S.R., Chandramouli, S., Premsai, T.P., Prithviraj, P., Vivek, M., Kishore, V.R. (2014). Numerical analysis of effect of pitch angle on a small-scale vertical axis wind turbine. *International Journal of Renewable Energy Research*, *4*(4), 929-935.

[2]　Guţu, M. (2017). *Optimizing the resistance structure of aerodynamic blades for wind turbines*. Doctoral thesis, Chisinau, Moldova.

[3]　Bychkov, N.M., Dovgal, A.V., Kozlov, V.V. (2007). Magnus wind turbines as an alternative to the blade ones, J. Phys.: Conf. Ser. 75 012004

[4]　Hameed, M.S., Afaq, S.K. (2013). Design and analysis of a straight bladed vertical axis wind turbine blade using analytical and numerical techniques*, Ocean Engineering, 57,* 248–255.

[5]　Jang, H., Paek, I., Kim, S., Jeong, D. (2019). Performance prediction and validation of a small-capacity twisted Savonius wind turbine, *Energies, 12,*17-21.

[6]　Mara, B.K., Mercado, B.C., Mercado, L.A., Pascual, J.M., Lopez, N.S. (2014). Development and validation of a CFD model using ANSYS CFX for aerodynamics simulation of Magnus wind rotor blades, *Proceedings of 7th International Conference Humanoid, Nanotechnology, Information Technology Communication and Control, Environment and Management (HNICEM), Palawan, Philippines.*

[7]　Nigam, P.K., Tenguria, N., Pradhan, M.K. (2017). Analysis of horizontal axis wind turbine blade using CFD, *International Journal of Engineering, Science and Technology, 9* (2), 46-60.

[8]　Paulsen, U.S., Madsen, H.A., Hattel, J.H., Baran, I., Nielsen, P.H. (2013). Design optimization of a 5 MW floating offshore vertical-axis wind turbine, *Energy Procedia, 35,* 22-32.

[9]　Rogowski, K., Maronski, R., Piechna, J. (2015). Numerical analysis of a small-size vertical-axis wind turbine performance and averaged flow parameters around the rotor, *Archive of mechanical engineering*, *LXIV* (2), 205-218.

[10]　Tudor, C.I. (2015). *Research regarding the implementation, adaptation and functioning of the wind turbines for small consumers,* Doctoral thesis, Brasov, Romania.

[11]　Wenehenubun, F., Saputra, A., Sutanto, H. (2015). An experimental study on the performance of Savonius wind turbines related with the number of blades, *Energy Procedia*, 68, 297–304;

[12]　Wußow, S., Sitzki, L., Hahm, T. (2007). 3D-simulation of the turbulent wake behind a wind turbine, *Journal of Physics Conference Series*, *75* (1), 012033.